Environmental Pollution 238 (2018) 903–917

Contents lists available at ScienceDirect

Environmental Pollution

journal homepage: www.elsevier.com/locate/envpol

Impacts of transportation sector emissions on future U.S. air quality in a changing climate. Part I: Projected emissions, simulation design, and model evaluation☆

Patrick Campbell [a], Yang Zhang [a, *], Fang Yan [b, c, d], Zifeng Lu [b, c], David Streets [b, c]

[a] Department of Marine, Earth, and Atmospheric Sciences, NCSU, Raleigh, NC, 27695, USA
[b] Computation Institute, University of Chicago, Chicago, IL, 60637, USA
[c] Energy Systems Division, Argonne National Laboratory, Argonne, IL, 60439, USA
[d] Currently at Mobile Source Control Division, California Air Resources Board, Sacramento, CA, 95814, USA

ARTICLE INFO

Article history:
Received 6 December 2017
Received in revised form
14 February 2018
Accepted 3 April 2018
Available online 17 April 2018

Keywords:
WRF/CMAQ
Transportation sector emissions
Technology driver model
SPEW-Trend
Climate change
Dynamical downscaling

ABSTRACT

Emissions from the transportation sector are rapidly changing worldwide; however, the interplay of such emission changes in the face of climate change are not as well understood. This two-part study examines the impact of projected emissions from the U.S. transportation sector (Part I) on ambient air quality in the face of climate change (Part II). In Part I of this study, we describe the methodology and results of a novel Technology Driver Model (see graphical abstract) that includes 1) transportation emission projections (including on-road vehicles, non-road engines, aircraft, rail, and ship) derived from a dynamic technology model that accounts for various technology and policy options under an IPCC emission scenario, and 2) the configuration/evaluation of a dynamically downscaled Weather Research and Forecasting/Community Multiscale Air Quality modeling system.

By 2046–2050, the annual domain-average transportation emissions of carbon monoxide (CO), nitrogen oxides (NO_x), volatile organic compounds (VOCs), ammonia (NH_3), and sulfur dioxide (SO_2) are projected to decrease over the continental U.S. The decreases in gaseous emissions are mainly due to reduced emissions from on-road vehicles and non-road engines, which exhibit spatial and seasonal variations across the U.S. Although particulate matter (PM) emissions widely decrease, some areas in the U.S. experience relatively large increases due to increases in ship emissions. The on-road vehicle emissions dominate the emission changes for CO, NO_x, VOC, and NH_3, while emissions from both the on-road and non-road modes have strong contributions to PM and SO_2 emission changes. The evaluation of the baseline 2005 WRF simulation indicates that annual biases are close to or within the acceptable criteria for meteorological performance in the literature, and there is an overall good agreement in the 2005 CMAQ simulations of chemical variables against both surface and satellite observations.

1. Introduction

Rapid population growth, global urbanization, and advanced technologies have led to significant fluctuations in transport, fuel consumption, and emissions of greenhouse gases (GHG) and air pollutants over different world regions. Since the advent of the Clean Air Act in 1970, there has been reduced pollution from transportation sources for many areas of the U.S., in large part due to cleaner cars, trucks, and fuels (https://www.epa.gov). Between 1970 and 2014, the emissions of air pollutants such as volatile organic compounds (VOCs), nitrogen oxides (NO_x), carbon monoxide (CO), and particulate matter with an aerodynamic diameter < 10 μm (PM_{10}) are down by 87%, 64%, 86%, and 37%, respectively (DOT, 2016). Transportation emissions of PM with an aerodynamic diameter <2.5 μm ($PM_{2.5}$) are also down by 48% over the U.S. since 1970. The reductions in transportation emissions of air pollutants are in part due to more stringent light-duty engine and fuel standards in the U.S. Additional complexities arise, however, when disaggregating the past changes in transport modes and the coincident GHGs and air pollutants emitted. Current levels in

☆ This paper has been recommended for acceptance by David Carpenter.

* Corresponding author. Department of Marine, Earth, and Atmospheric Sciences, NCSU, Raleigh, NC, 27695, USA.
E-mail address: yzhang9@ncsu.edu (Y. Zhang).

https://doi.org/10.1016/j.envpol.2018.04.020
0269-7491/

U.S. GHG emissions from passenger cars, light-duty trucks, medium/heavy-duty trucks, and buses have increased compared to 1990 by about 16%, 1%, 76%, and 127% respectively; however, other transport modes such as commercial aircraft, ships/boats, and rail have mixed GHG emission trends of about a 5% increase, 36% decrease, and 22% increase respectively (EPA, 2016a). The combined emissions from both on-road vehicles and non-road engines may contribute a large percentage (~up to 41%) of the total smog-forming anthropogenic NO_x emissions, and thus it is very important to continue to study their future trends in different world regions (Yan et al., 2014).

Correlating with an expanding global population, possibly beyond 9.6 billion by 2050 (EEA, 2015), it is projected that significant growth in the number of vehicles (>1 billion) in the global transportation sector is expected to continue through 2050 (IEA, 2014). The relationship of future transport fuel consumption to emission changes is not linear, however, and the emission projections depend on dynamic relationships between socioeconomic drivers and technological changes. Recent global emission scenarios that are driven by the Intergovernmental Panel on Climate Change (IPCC) Special Report on Emission Scenarios (SRES) for the A1B scenario (Nakicenovic et al., 2000), predict a decline in transportation emissions of CO, NO_x, VOCs, and PM by 2030, but then an increase through 2040 due to the rapid increases in the number of on-road vehicles with minimal to no emission standards in Africa, as well as due to increasing emissions from non-road gasoline engines and shipping (Fig. 2 in Yan et al., 2014). Such global changes in emissions and air quality will affect the U.S., as both pollutants and precursors to pollutant formation can be transported to and from the U.S.

A technique to study such interconnections across the global-to-regional scale is through dynamically downscaling of global climate models (GCMs). Dynamical downscaling of GCMs is a technique that uses relatively coarse resolution initial and boundary conditions (ICONs/BCONs) from the GCM as driving fields to a regional numerical modeling system run at a spatially finer resolution. This technique has been well documented in the past (e.g., Leung et al., 2006), and is used to investigate current and future regional climate changes, as well as to infer the potential air quality responses over North America and the U.S. (Gao et al., 2012; Trail et al., 2013; Wang and Kotamarthi, 2015)

Downscaling GCMs using regional air quality models (AQMs) allows for novel investigations of the impacts of global changes on regional scale climate and air quality over the U.S., i.e., Regional Climate Models (RCMs), which has historically been used to investigate O_3 and $PM_{2.5}$ levels in current and future periods (Hogrefe et al., 2004; Tao et al., 2007; Nolte et al., 2008; Dawson et al., 2009; Weaver, 2009; Lam et al., 2011; Gao et al., 2013; Penrod et al., 2014; Gonzalez-Abraham et al., 2015), while other studies have expanded to looking at an extensive list of atmospheric pollutant changes and their aerosol-cloud-climate feedbacks (e.g., Yahya et al., 2017a; b). A past review of RCM studies show potential for future increases in summertime O_3 (1–10 ppb) over large regions of the U.S. (Jacob and Winner (2009) and references within); however, there are contrasts in the spatial variability of concentration change, as well as uncertainty in the direction of change across different simulations (Weaver, 2009). A recent study by Gonzalez-Abraham et al. (2015) used a downscaled RCM model driven with global and regional-scale changes of climate, biogenic emissions, land use, and anthropogenic emissions. They found that daily maximum 8-hr O_3 concentrations will increase between 2 and 12 ppb across most of the continental U.S. (CONUS) for an average future summer period of 2046–2054. Other work that has considered the impact of rigorously developed anthropogenic emission projections developed by groups at Massachusetts Institute of Technology, Northeast States for Coordinated Air Use Management, and the U.S. Environmental Protection Agency (EPA), have shown predominantly decreasing future primary pollutant levels over the U.S., which is largely due to decreases in precursor gases in the face of climate change (Fann et al., 2015; Garcia-Menendez et al., 2015; Rudokas et al., 2015).

RCM studies have also investigated the impacts of climate change on $PM_{2.5}$ concentrations and components (Avise et al., 2009; Pye et al., 2009; Lam et al., 2011), where the complexities of the secondary inorganic $PM_{2.5}$ components (e.g., sulfate (SO_4^{2-}), nitrate (NO_3^-), and ammonium (NH_4^+)) and organic carbon (OC) response to changes in meteorological drivers lead to additional uncertainties in $PM_{2.5}$ predictions ($\pm 0.1-1\ \mu g\ m^{-3}$) that are further discussed in Jacob and Winner (2009) and Tai et al. (2010). Gonzalez-Abraham et al. (2015), however, found that $PM_{2.5}$ levels may increase by between 4 and $10\ \mu g\ m^{-3}$ in the Northeast, Southeast, Midwest, and South regions of the U.S. Much of the variability between different RCM studies comes from the uncertainties in the models' approximations of physical and chemical processes in the atmosphere; however, further model error stems from uncertainty in RCM inputs that include the meteorological and chemical ICONs/BCONs, and quite importantly the emissions and their projection methods.

In a study on near-future (2026–2030) U.S. air quality, Penrod et al. (2014) used an offline Weather Research and Forecasting (WRF; Skamarock and Klemp, 2008; Skamarock et al., 2008) model and Community Multiscale Air Quality (CMAQ; Byun and Schere, 2006) modeling system (hereafter WRF/CMAQ) that was driven by ICONs/BCONs from the National Center for Atmospheric Research (NCAR) Community Climate System Model (CCSM). The WRF model has been used extensively in dynamically downscaled regional climate simulations, where its applicability and limitation were well summarized in Leung et al. (2006). The Penrod et al. (2014) simulations incorporated domain-uniform/lumped growth factors (GFs) for future anthropogenic emissions (all sources/sectors), which were developed by Argonne National Laboratory (ANL), and based on the IPCC A1B scenario. Results showed that future U.S. air quality is characterized by mainly decreases in O_3 due to decreasing NO_x emissions, except in the eastern U.S., where increased temperature leads to increased O_3. Future concentrations of $PM_{2.5}$ and many of its components are projected to decrease, due to decreases in emissions of primary pollutants (which lead to decreased concentrations of primary and secondary anthropogenic pollutants), as well as increased precipitation in the winter. Considering that the emission projections in Penrod et al. (2014) and Gonzalez-Abraham et al. (2015) are domain-uniform and U.S.-uniform, respectively, the state-level spatial variability in the projected emissions across the U.S. is not accounted for. Ran et al. (2015) developed a robust region-to-county GF disaggregation and county-to-grid allocation (i.e., updating spatial surrogates) approach for non-power sector emission projections, and showed that it can represent future population density and land use changes in more detail, thus impacting future spatial variability in emissions and important air quality variables. The emission projections in the aforementioned studies, however, neglected considerable detail regarding the technology stock and explicit relationships that exist between socioeconomic drivers and technological changes in the transportation sector. In fact, due the effects of stringent emission standards (i.e., technology) offsetting the impending growth in fuel consumption, Yan et al. (2014) projected global transportation emissions to initially decrease in the near-future, 2026–2030, but then to increase in some scenarios by 2046–2050.

Part I of this sequence of papers first describes the methodology of a novel Technology Driver Model (TDM; see graphical abstract),

which includes the model configuration and simulation design of the downscaled WRF/CMAQ model component used in the TDM approach (Section 2). While previous studies mainly show impacts of domain-uniform/lumped emission projections with no explicit technological impacts, this paper next describes the advanced emission projection development for the transportation sector using a dynamic technology model based on the Speciated Pollutant Emission Wizard (SPEW)-Trend model, while further quantifying the transportation emission projections over the U.S. (Section 3). The results from baseline 2005 WRF/CMAQ simulations and a comprehensive evaluation are then discussed (Section 4) to show confidence in the WRF/CMAQ modeling system used in the TDM approach to simulating the 5-year current (2001–2005) and future (2046–2050) periods in Part II of this work, which quantifies the impacts of the transportation emission changes on future U.S. air quality in the face of climate change. Lastly, we present a summary and discussion of the results (Section 5). To the authors knowledge, such a TDM approach of using novel technology-driven transportation emission projections into global-to-regional downscaled WRF/CMAQ simulations to study future U.S. air quality has not previously been investigated, and serves to aid in future transportation air quality regulation and control, as is further discussed in Part II of this work (Campbell et al., 2018).

2. Methodology

2.1. The Technology Driver Model (TDM) approach

The collaborative TDM approach first uses exogenous IPCC SRES scenarios (in this work the A1B scenario) that provide socioeconomic variables as inputs to explicit relationships that affect technological changes, and predict global-to-regional energy use and fuel consumption. The derived relationships between socioeconomic and technological changes are implemented in a dynamic technology model for the transportation sector known as the Speciated Pollutant Emission Wizard-Trend (SPEW-trend), which is capable of predicting the distribution of vehicle (and engine) fuel consumption by region, fuel type, technology, and age (i.e., technology splits). The SPEW-Trend model combines the fuel consumption information with a distribution of emission factors by species, fuel, technology, and age to develop global and regional emission projections. More details on the SPEW-Trend model are provided in Section 3.1. Emission GFs for a chosen baseline year are generated from the dynamic technology emission projections (Section 3.1), and are further processed with a regional emission inventory to generate gridded emissions that are model-ready for the RCM (i.e., WRF/CMAQ; Section 3.2) used in climate-air quality model predictions (Part II).

The transportation emission projections from SPEW-Trend (Yan et al., 2014) are quite different than other regional emission projection methodologies, such as a recently developed emissions inventory and future 2040 projections done in support of air quality modeling completed by the U.S. EPA, known as the Heavy Duty Vehicle Greenhouse Gas (HDGHG) Phase 2 rule (hereafter EPA projections) that establish fuel efficiency and greenhouse gas emissions standards for commercial medium-and heavy-duty on-highway vehicles and work trucks beginning with the 2018 model year (EPA, 2016b). The EPA projections to 2040 include future changes in the onroad, nonroad, locomotive, commercial marine vessels (CMVs), and aircraft sectors for the Criteria Air Pollutants (CAPs), and are generally based on a combination of model-based (onroad and nonroad) and data-estimated (locomotive, CMVs, and aircraft) control strategies and growth assumptions. The EPA projections are strongly driven by nationally modeled onroad and nonroad sector rules, which included more stringent vehicle emissions and fuel standards in the future (EPA, 2016b). The EPA onroad projections are modeled using EPA's MOtor Vehicle Emission Simulator (MOVES) model, and contains a number of CONUS states that adopt more stringent California Tier-3 emissions and fuel standards. The EPA nonroad projections also contain the "Clean Air Nonroad Diesel Final Rule - Tier 4" standards. Thus the SPEW-Trend projections are somewhat limited in that they do not contain the advanced post-Tier 2 standards (see Section 3) as compared to the EPA projections; however, the EPA projections lack the dynamic relationships between socioeconomic factors and technological changes modeled explicitly in SPEW-Trend (Section 3) (Yan et al., 2011, 2014). Ideally, an emission projection dataset that harmonizes these aspects would be most advantageous in future air quality projections.

2.2. Model configuration and design summary

This work uses the WRF version 3.6.1 and (offline) CMAQ version 5.0.2 (doi:10.5281/zenodo.1079898). There are two sets of WRF simulations performed in this work: one for the current 2001–2005 and future 2046–2050 climate periods, using downscaled CCSM-based meteorological ICONs and BCONs (hereafter WRF_CCSM) for the A1B scenario, and another for a model baseline evaluation during one current year (2005), which uses National Center for Environmental Prediction (NCEP) Final (FNL) operational global analysis data on $1^\circ \times 1^\circ$ grids prepared operationally every 6 h for meteorological ICONs and BCONs (hereafter WRF_NCEP). The domain of the WRF/CMAQ simulations includes CONUS (centered at 39.3°N and 97.6°W) and parts of Canada and Mexico at a horizontal resolution of 36×36 km resolution. The major WRF model attributes are the 1) revised Monin-Obukhov surface layer scheme, 2) Unified Noah land surface model with urban canopy physics, 3) Yonsei University planetary boundary layer scheme, 4) Rapid Radiative Transfer Model for GCMs for shortwave and longwave radiation, 5) Morrison Double-Moment grid-scale microphysics scheme, and 6) Grell-Freitas Ensemble sub-grid cumulus physics parameterization (see Table S1 for scheme references). The Carbon Bond Mechanism 2005 with updated toluene and activated chlorine chemistry (CB05-TUCL; Table S1), and the CMAQ Aerosol Module Version 6 (AERO6; Table S1) are used for the gas-phase chemistry and aerosol modules, respectively. Current period anthropogenic emissions are based on U.S. EPA's NEI 2005v4, and future period emissions are based on SPEW-Trend transportation emission projections (Section 3.2). The WRF/CMAQ simulation design is divided into a 2005 base year for evaluation and comparison (NCEP- vs. CCSM-driven WRF), a current year period 2001–2005, and six main sensitivity simulations for the future period 2046–2050 that investigate the impacts of 1) on-road vehicle (ORV) emission changes, 2) non-road engine (NRE) emission changes, 3) total transportation (TT) emission changes, and 4) the interplay among TT emission, GHG, and climate changes, all for the IPCC A1B scenario (Part II; Section 3 in Campbell et al., 2018). Table S1, Fig. S11, and supporting discussion provide more relevant details on the full physics and chemistry model configuration, other model attributes (e.g., inline CMAQ emission models/references), domain boundaries, and other design details.

3. Dynamic technology-driven transportation emissions

3.1. The SPEW-Trend projection model

The future emissions of ORVs and NREs in this work are estimated by SPEW-Trend, which is a hybridization of an engineering ("bottom-up") and economic ("top-down") model (Yan et al., 2011). SPEW-Trend is driven by future estimates of variables such as fuel

consumption, population, and gross domestic product that are taken from the integrated assessment model known as the Integrated Model to Assess the Global Environment (IMAGE) developed for IPCC SRES (Nakicenovic et al., 2000). Emission characteristics in the model are assigned to 17 world regions and the U.S. is one of them. SPEW-Trend is different from other emission projection models, as it applies dynamic relationships between socioeconomic factors and technological changes to determine future emissions. The details about the SPEW-Trend model applicability, robustness, and results of detailed transportation emission projections are described in Yan et al. (2011, 2014). We note that while SPEW-Trend transportation emission projections are available for four of the IPCC SRES (i.e., A1B, A2, B1, B2), in this work we focus solely on the A1B scenario, which allows for a more detailed investigation of the six sensitivity simulations noted in Section 2. While the choice of the A1B scenario may appear arbitrary, it is thought to be a conservative, or upper-limit approach to the transportation emission projections (see Fig. 2 of Yan et al., 2014). Furthermore, the A1B scenario is a rather balanced prediction, and does not rely too heavily on one particular energy source. Additional work investigating the SPEW-Trend emission projections for the B2 scenario (near the lower SPEW-Trend emission limit) is ongoing, where the impacts on future U.S. air quality and climate change will be further compared against the A1B scenario (Jena et al., 2018; Wang et al., 2018).

SPEW-Trend contains formulations that represent how ORVs or NREs retire with age and regional income level, the regional dependence of timing of new emission standards, the changes of emission factors for individual vehicles with age, and the effects of vehicle age on the fraction of normal emitters that become super-emitters (Yan et al., 2011). In the model, fleet dynamic changes are assumed to follow historical patterns, in the absence of evidence to the contrary. Any air-quality regulations other than the implementation of emission standards are not considered.

Future emissions from other transportation modes such as ship, rail, and aircraft are based on a combination of fuel consumption data and emission factors from previous literature, and no explicit technological changes are considered for these modes. The emission projections for these modes are determined by time-dependent, fleet-average emission factors obtained from other studies, which represent technological changes implicitly (Yan et al., 2014). The major implication from using such an "expert judgment" assumption for these transportation modes is a lack of consistency with the dynamic technological changes used in projecting the ORVs and NREs. Further information needs to be gathered about the factors that drive technology preferences, and the retirement decision-making for ships, aircraft, and locomotives to improve their consistency with the other transportation modes (see Section 5.2.2 of Yan et al., 2014).

Up to this point we have summarized the transportation emission historical and future projection methodologies of Yan et al. (2011, 2014), which pertain to a global and regional scale. Yan et al. (2014) provides numerous figures, tables, and discussion in their main text and supplementary material that quantify the global, region, and transportation mode specific results for total fuel consumption and emission magnitude changes for CO, NO_x, VOCs, and PM. Thus we refer the reader to Yan et al. (2014) for additional details, and any further information on the specific 1) data sources and assumptions used for historical and future fuel consumption, 2) timing of future emission standards, 3) emission intensity of CO and VOC for NREs, and 4) other assumption details.

3.2. Regional and state allocation methodology for the U.S.

Emission projections in the U.S. are further allocated to each contiguous state based on the energy consumption at state level. Energy consumption estimates from the State Energy Data System (SEDS) are used for the past and current, and these estimates are then projected using business-as-usual trends reported in the Department of Energy (DOE) 2013 Annual Energy Outlook (AEO 2013) (DOE, 2013) and scaled using the IPCC SRES for the U.S. Using known technological and demographic trends, a reference scenario provides energy-use projections by sector and energy source for nine U.S. census regions (i.e., New England, Middle Atlantic, East North Central, West North Central, South Atlantic, East South Atlantic, West South Central, Mountain, and Pacific) from 2011 to 2040. For the reference scenario, the regional AEO2013 energy use forecasts are used directly and estimate the total energy consumed in each region for years 2041–2050 as:

$$TEC_{r,y} = \frac{\sum_{i=y-1}^{y-5} PEC_{r,i}}{5} \cdot TPO_{r,y} \quad (y = 2041,\ 2042, \ldots 2050), \qquad (1)$$

where r and y represent the region and the year, respectively. *TEC* is the total energy consumption; *PEC* is the per capita energy consumption; and *TPO* is the total population. Assuming the energy structure of region r in year y is the average of the previous five years, energy data (E) for fuel/energy source k in sector l can be calculated by:

$$E_{r,y,k,l} = \frac{\sum_{i=y-1}^{y-5} E_{r,i,k,l}}{\sum_{i=y-1}^{y-5} \mathrm{TEC}_{r,i}} \cdot \mathrm{TEC}_{r,y} \quad (y = 2041,\ 2042, \ldots 2050). \qquad (2)$$

The AEO2013 provides information on U.S. energy use of more than 50 fuels/energy sources in the major sectors (i.e., the commercial, industrial, residential, transportation, and electricity generation sectors) at the state level. For the transportation sector in this work, we incorporate the fuels/energy sources used in ORVs including light-duty-diesel (LDDV), heavy-duty diesel (HDDV), and light-duty gasoline (LDGV), and those from NREs including diesel and gasoline (for both two-stroke and four-stroke engines). For ship, rail, and aircraft we use energy sources of total (gasoline + diesel), diesel, and aviation gasoline respectively.

To disaggregate the projected regional energy estimates to the U.S. states, it is further assumed that the energy distribution among states of region r is the average distribution in the previous five years:

$$E_{s,y,k,l} = \frac{\sum_{i=y-1}^{y-5} E_{s,i,k,l}}{\sum_{i=y-1}^{y-5} E_{r,i,k,l}} \cdot E_{r,y,k,l} \quad (y = 2011, 2012, \ldots 2050), \qquad (3)$$

where s represents the state in region r. Through Equations (1)–(3), the reference energy consumption database by state, sector, and energy source was developed for the period of 2011–2050.

The reference scenario is also scaled to the IPCC SRES, which are formulated by IMAGE (Alcamo, 1994). IMAGE provides the U.S. primary and secondary energy use in major sectors under different IPCC scenarios for the whole period of 1971–2100. The energy use trend of the IPCC A1B scenario is followed at the national level for the period of 2011–2050. The U.S. national energy data (E_{US}) for energy source k in sector l year y is then corrected by:

where E'_{US} is the original U.S. energy data in the IPCC scenario *A1B*. State level energy data for scenario m is then scaled based on the reference scenario using the following equation:

$$\begin{cases} E_{\mathrm{US},y,k,l,A1B} = \dfrac{E'_{\mathrm{US},y,k,l,A1B}}{E'_{\mathrm{US},y-1,k,l,A1B}} \cdot E_{\mathrm{US},y-1,k,l,A1B} \quad (y = 2011, 2012, \ldots 2050), \\ E_{\mathrm{US},2010,k,l,A1B} = E_{\mathrm{US},2010,k,l,\mathrm{reference}} \end{cases} \tag{4}$$

$$E_{s,y,k,l,A1B} = \frac{E_{s,y,k,l,\mathrm{reference}}}{E_{\mathrm{US},y,k,l,\mathrm{reference}}} \cdot E_{\mathrm{US},y,k,l,A1B} \quad (y = 2011, 2012, \ldots 2050). \tag{5}$$

Fig. 1 compares the total energy consumption projected in the U.S., and for the states of North Carolina and California under the IPCC A1B scenario. The spatial distribution of total energy consumption by state in 2050 is further shown in Fig. 2.

There is significant spatial inhomogeneity in the distribution of total energy consumption across the U.S., and this has an impact on the state allocation of projected transportation emissions.

With the projected state level energy consumption, the total emissions in the U.S. can be allocated to each state by:

$$Emiss_{s,y,k,l,A1B} = \frac{\mathrm{Emiss}_{US,y,k,l,\mathrm{A1B}}}{\sum_s E_{\mathrm{s},y,k,l,\mathrm{A1B}}} \cdot E_{\mathrm{s},y,k,l,A1B} \quad (y = 2011, 2012, \ldots 2050). \tag{6}$$

Emission GFs are defined as the ratio of emissions in future years and a base year. In this study, they are calculated using the emissions for 2046–2050 relative to a base year of 2005 for CO, methane (CH_4), nitrogen oxide (NO), nitrogen dioxide (NO_2), nitrous oxide (N_2O), ammonia (NH_3), sulfur dioxide (SO_2), total PM (including $PM_{2.5}$ and PM_{10}), elemental carbon (EC), OC, and total non-methane VOCs. Consequently, the emission GFs are specific to each future year, scenario, species, U.S. state, transportation mode, and fuel type, and to our knowledge represent the most comprehensive transportation emission projections to year 2050 over CONUS.

We note that emission projections from SPEW-Trend are based on assumptions of vehicle fleet dynamics that follow historical patterns, and it does not include impacts from current transformational changes in the U.S. transportation sector such as autonomous and electric vehicles, and new ride sharing technologies. Some of these aspects, however, are indirectly accounted for by the rapid introduction of new and more efficient technologies in the IPCC A1B scenario, and use in scaling the reference scenario in Eq. (4). Results from Liu and Lin (2017) further indicate that the market future for plug-in electric vehicles is highly uncertain, and that the top factors contributing to this uncertainty are price sensitivities, energy cost, range limitation, and charging availability. Given the uncertainty in the long-term market future for electric vehicles, SPEW-Trend emission projections to 2046–2050 remain vital to our understanding of future air pollution changes, while further aiding regulatory planning and air pollution mitigation strategies in the event that electric vehicles, and other alternative transportation technologies/methodologies, are not widely embraced in future U.S. transportation management strategies. If alternative transportation technologies make a significant impact on reducing emissions over the long-term in the U.S., then the SPEW-Trend projections to 2046–2050 shown here remain a conservative baseline for future impact assessments.

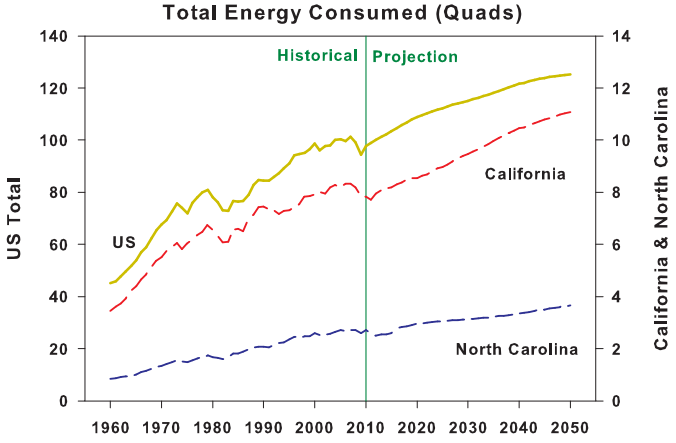

Fig. 1. Total energy consumption for the U.S. (solid yellow), North Carolina (dashed blue), and California (red) under the IPCC A1B scenario for 1960–2050. (For interpretation of the references to color in this figure legend, the reader is referred to the Web version of this article.)

Table 1 and Fig. 3 summarize the U.S. average 2005 and 2046–2050 transportation sector emission magnitudes (and percent changes), and the GF percent change ((GF-1)*100%) by each transportation emission sector and fuel for SPEW-Trend emission species CO, NO_x, anthropogenic VOC (AVOC), SO_2, NH_3, and PM under the A1B scenario.

The average GF was calculated across all U.S. states for each year of 2046–2050, and the 5 yearly values are averaged. The total PM ($PM_{2.5} + PM_{10}$) emission changes are very similar to the changes for the EC and OC species, and thus EC and OC are not shown. Fig. 3 shows clear differences in the emission changes between different species across the different transportation modes. When summed over the different fuel types, Table 1 shows decreases in the ORV, NRE, and total transportation emissions by 2046–2050 for all SPEW-Trend emission species; however, there are contributions from increases in all species for the ship and aircraft mode (except for NH_3). There are also increases in NH_3 rail emissions, but their contribution is small due to the very small magnitude of rail relative to the total transportation sector emissions.

The average emissions of CO, NO_x, VOC, and SO_2 show decreases for the non-road diesel engines and on-road vehicles (LDDV, HDDV, and LDGV) by 2046–2050 (Fig. 3a–d) in part because vehicles still follow Tier 2 (2007–2010) standards during 2046–2050, which are at least more stringent than the standards during base year 2005. The emission decreases for on-road vehicles are also impacted by decreases in fuel consumption for LDDV and LDGV (U.S. avg. ~31% decrease for both; Fig. 3a) that are larger than the increases in fuel consumption for HDDV (U.S. avg. ~15% increase; not shown). The decrease in CO, NO_x, VOC, and SO_2 for non-road diesel engines are due to larger emission factor reductions compared to increases in fuel consumption for this transportation mode (Yan et al., 2014). The average non-road diesel engine emissions of CO, NO_x, VOC, and SO_2 have percentage decreases of about 40%, 72%, 69%, and 100% by 2046–2050, respectively. For on-road vehicles, the largest decreases in CO and VOC emissions are from the LDDV mode, the largest decreases in NO_x are found mainly in the HDDV classification, and for SO_2 there are nearly equally large decreases in LDGV, LDDV, and HDDV. The total on-road emissions of CO, NO_x, VOC, and SO_2 decrease by about 44%, 67%, 45%, and 96%, respectively. Average emissions of VOCs, however, increase for non-road gasoline engines by about 20%, and only very slightly decrease for CO by about 1% (Fig. 3b and d). This is because emission control of non-road gasoline engines is not as stringent as for on-road and there is

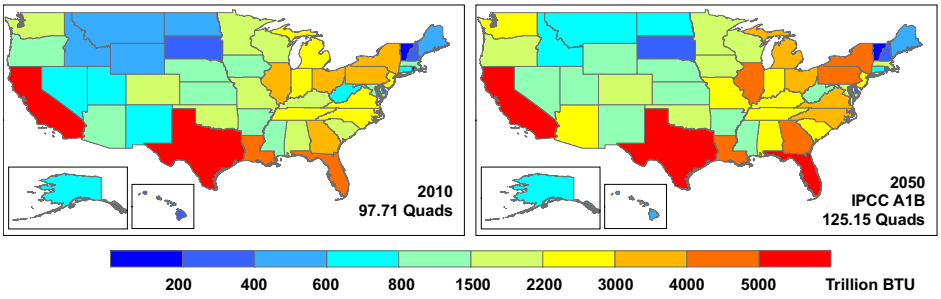

Fig. 2. Distribution of total energy consumption by state in a) 2010, and b) for the IPCC A1B scenario in 2050.

Table 1
SPEW-Trend yearly gas (CO, NO_x, AVOCs, SO_2, and NH_3) and PM emission magnitudes for 2005 and the average of 2046–2050 for the ORV, NRE, ship, rail, and aircraft modes, as well as the total transportation (summed over different fuels for each transportation mode). Values in parenthesis for 2046–2050 represent the percent (%) change, and are colored red for increases and blue for decreases. Emission magnitudes are in units of Tg yr^{-1}, and are rounded to two decimal places.

Species	2005						Ave. 2046 – 2050 (% Change)					
	ORV	NRE	Ship	Rail	Aircraft	Total	ORV	NRE	Ship	Rail	Aircraft	Total
CO	8.84	4.52	0.13	0.14	0.72	14.34	5.85 (-33.79)	4.05 (-10.31)	0.19 (49.65)	0.08 (-42.86)	0.72 (1.01)	10.89 (-24.01)
NO_x	3.14	1.10	1.81	0.80	1.04	7.89	0.98 (-68.76)	0.33 (-70.07)	2.00 (10.39)	0.26 (-67.34)	2.00 (91.59)	5.57 (-29.42)
AVOCs	0.77	0.35	0.12	0.10	0.12	1.46	0.54 (-30.41)	0.31 (-10.68)	0.16 (36.62)	0.06 (-39.19)	0.07 (-40.78)	1.15 (-21.73)
SO_2	0.38	0.03	1.17	0.12	0.06	1.76	0.02 (-95.03)	0.00 (-95.14)	1.50 (28.82)	0.00 (-99.53)	0.16 (153.58)	1.68 (-4.46)
NH_3	0.16	0.00	0.00	0.00	n/a	0.16	0.05 (-65.30)	0.00 (-0.20)	0.00 (49.65)	0.00 (55.47)	n/a (n/a)	0.06 (-63.52)
PM	0.08	0.10	0.15	0.05	0.00	0.39	0.05 (-43.84)	0.03 (-69.98)	0.20 (36.62)	0.01 (-89.24)	0.01 (153.58)	0.29 (-25.70)

greater use of non-road gasoline engines in the future. Thus the effects of increasing non-road gasoline fuel consumption (U.S. avg. ~29% increase; Fig. 3a) in the future could overcome the effects of emission factor reduction by implementations of more stringent standards for some species including CO and VOCs (Yan et al., 2014). Non-road diesel emissions of NH_3 increase significantly by about 153%, while non-road gasoline and on-road LDDV, HDDV, and LDGV emissions of NH_3 decrease by 12%, 20%, 32%, and 66%, respectively (Fig. 3f). We note that the Greenhouse gas - Air pollution Interactions and Synergies (GAINS) model (http://gains.iiasa.ac.at/) used to derive NH_3 emission factors for non-road diesel engines are a rough approximation, and although there is a large increase it will not affect the total non-road emissions significantly. The PM emissions decrease by about 83%, 82% and 45% for the non-road diesel, on-road LDDV, and on-road HDDV modes, respectively, but increase by about 53% and 13% for the non-road gasoline and on-road LDGV modes, respectively (Fig. 3g).

Emission projections from the ship, rail, and aircraft modes do not contain explicit technological-changes; however, their fraction of the total transportation sector emissions may be considerable in some regions of the U.S. Shipping and aircraft are international activities, however, and thus their regional comparisons are only approximate. The ship emissions increase for all species, except for NH_3, which does not change in the future (Fig. 3f). The changes in ship emissions in Fig. 3 are consistent with globally increasing emissions from ships by 2046–2050, which are largely due to increases in global fuel consumption dominating the decreases in emission factors due to more stringent emission standards for this transportation mode (Yan et al., 2014). Thus it follows that the U.S. has large increases in fuel consumption for ships in the future (Fig. 3a). The U.S. average ship emissions range from an increase of 231% (NO_x) to about 349% (CO). For rail there are increased emissions for CO, NO_x, VOCs, and NH_3 (Fig. 3b–d and f), but decreased emissions for SO_2 and PM (Fig. 3e and g). The increased emissions for CO, NO_x, and VOCs are modest to major, ranging from 22% to 127%, while the increased emission for NH_3 is extreme at about 480%. The future emission factors decrease for CO, NO_x, and VOCs with tighter future standards; however, their changes are

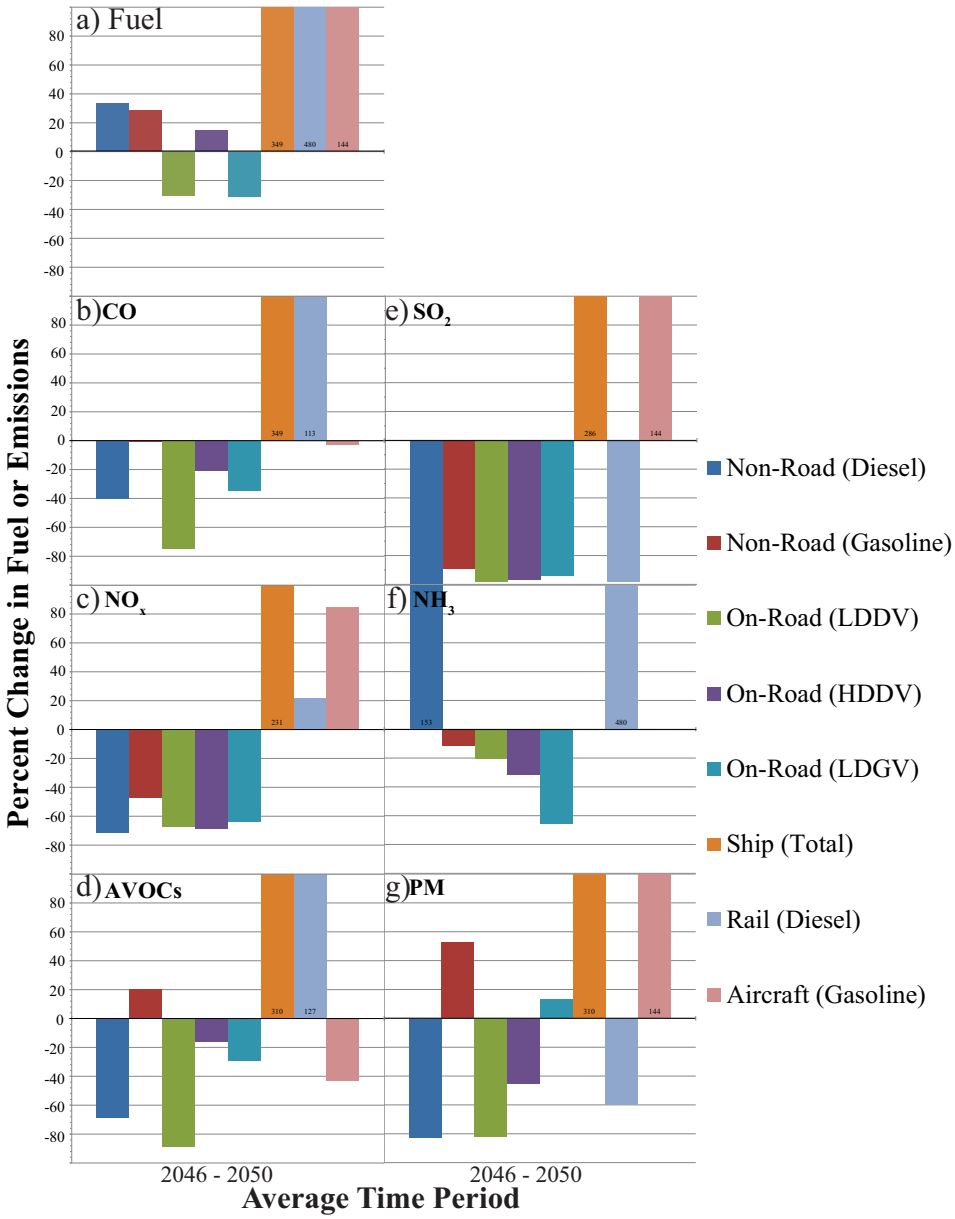

Fig. 3. U.S. average percent changes for a) fuel consumption, and emissions of b) CO, c) NO_x, d) anthropogenic VOCs (AVOCs), e) SO_2, f) NH_3, and g) PM under the A1B scenario for an average 2046–2050 time period relative to 2005. The different transportation modes are color coded according to the legend on the right. Total PM ($PM_{2.5} + PM_{10}$) emission changes represent similar changes for the EC and OC species (not shown). NH_3 emissions do not change for the ship and aircraft modes for all future years. Emission changes > + 100% show their value at the base of each respective column. (For interpretation of the references to color in this figure legend, the reader is referred to the Web version of this article.)

overcompensated by larger increases in fuel consumption (Fig. 3a), which are projected by gross domestic product changes for this transportation mode (Yan et al., 2014). The rail SO_2 and PM emissions, however, decrease by about 98% and 60%, respectively. There are increases of aircraft gasoline emissions for NO_x, SO_2, and PM (Fig. 3c, e, and 3g), and decreased emissions for CO and VOC emissions (Fig. 3a and c). The increase in aircraft emissions range from 85% (NO_x) to 144% (SO_2 and PM), while the decreased emissions range from 3% (CO) to 43% (VOCs). The increases in NO_x and PM for aircraft are due to very small decreases in emission factors compared to much larger increases in fuel consumption (Fig. 3a), while the slight to moderate decreases for CO and VOCs are due to larger decreases in emission factors that overcompensate fuel consumption increases (Yan et al., 2014). The SO_2 emissions from aircraft are relatively very small, and their emission factors are based on one single value that depends on aircraft gasoline sulfur content. The ship and aircraft NH_3 emission factors taken from GAINS and used in Yan et al. (2014) are based on a single constant value and thus neither transportation modes are projected for NH_3. The large increases in NH_3 for rail are rather approximate, and we note that its contribution to the total transportation changes in NH_3 remains quite small.

The states of California (CA) and North Carolina (NC) have rather different projections in energy and fuel consumption (Figs. 1 and 2). Thus, Fig. 4 provides an example comparison of the state-level CA and NC differences in percent emission changes by 2046–2050.

There are clear differences in the emission changes between NC and CA. NC has larger (smaller) percent emission decreases (increases) for all species in the non-road diesel, rail, and aircraft modes, indicating lesser emissions from these modes for NC

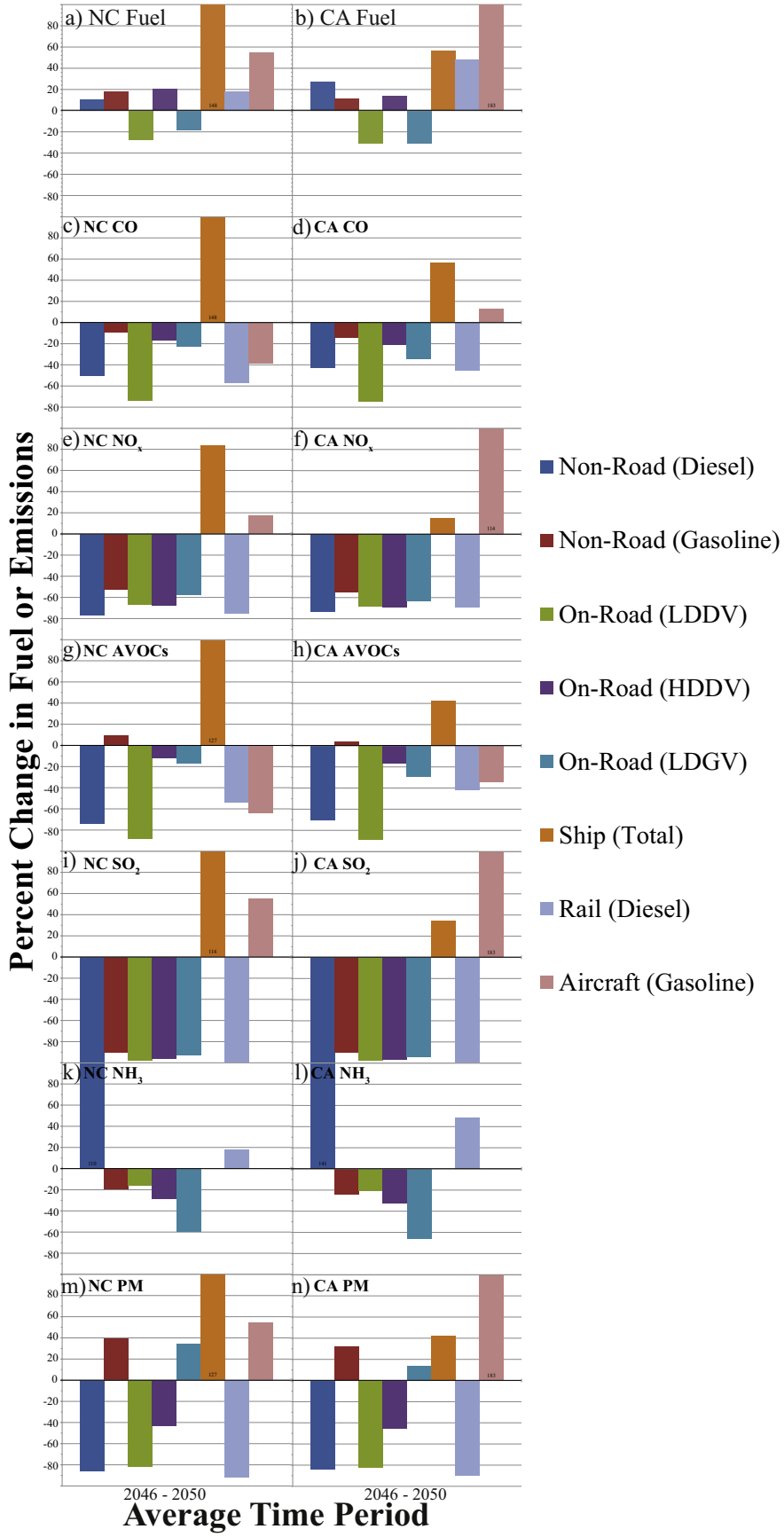

Fig. 4. North Carolina (left) and California (right) average percent changes of a) – b) fuel consumption, and emissions of c) – d) CO, e) – f) NO_x, g) - h) AVOCs, i) – j) SO_2, k) – l) NH_3, and m) - n) PM under the A1B scenario for an average 2046–2050 time period relative to 2005. Other details are the same as described in Fig. 3.

compared to CA in the future. This result agrees with the smaller overall fuel consumption increases for NC compared to CA by 2046–2050 on average for these modes (Fig. 4a and b). There are, however, greater non-road gasoline and on-road LDDV, HDDV, and LDGV emissions in the future for all species in NC, in part due to either larger (smaller) increases (decreases) in future fuel consumption in these modes. Furthermore, NC has far greater emissions from the ship mode in the future impacted by much larger (~by a factor of 3) increases in fuel consumption in this mode. To our knowledge, such state-level spatial variability for future transportation emission projections over the U.S. that include dynamic technological changes has not been previously investigated.

The gas-phase mechanism used in the version of CMAQ available for this project (Section 2.2) does not account for dynamically changing CH_4, CO_2, or N_2O emissions, and thus the SPEW-Trend emissions are not used (nor shown) here for these species, but rather the CH_4 and CO_2 background concentrations are prescribed in the future for the A1B scenario. Future CH_4 and CO_2 concentrations are based on projected values from 1990 taken from Nakicenovic et al. (2000), which is qualitatively similar to a projection from 2005 (see Fig. 5 in Nakicenovic et al., 2000). Based on the values shown in Table 3a of Nakicenovic et al. (2000), in 1990 the CH_4 emissions are about 310 Mt/yr, while in 2050, the CH_4 emissions range from 452 to 636 Mt/yr, with an estimated mean value 544 Mt/yr for the A1B scenario. The percent change in emissions ranges from 45.5% to 105.2%, with a mean value of 75.5%, or rather a GF of 1.8, and thus a future background CH_4 concentration of 1.85 ppm*1.8 = 3.33 ppm. The CO_2 emissions in 1990 and 2050 for A1B are 7.1 GtC/yr and 16.4 (average of range 12.7–26.7) GtC/yr, which results in a GF of 2.3, and thus a future background CO_2 concentration of 340 ppm*2.3 = 785.4 ppm. N_2O is not a reactant in the gas-phase mechanism or aqueous chemistry in this version of CMAQ (Section 2.2), and its background concentration does not change in the future.

3.3. Emissions processing and application

The emissions are based on criteria and hazardous pollutant emission inventories from the highly detailed EPA's 2005 National Emissions Inventory (NEI) Version 4 (http://www.epa.gov/ttn/chief/net/2005inventory.html#inventorydata). This version of the platform consists of CAPs and Hazardous Air Pollutants (HAPs) (including mercury (Hg), chlorine (Cl), and hydrochloric acid (HCl)) and benzene, acetaldehyde, formaldehyde, and methanol (BAFM). It is referred to as Version 4 because it has been updated from the 2002-based platform, Version 3 (EPA, 2010). To prepare the spatially, temporally, and chemically speciated model-ready emissions, we use the Sparse Matrix Operator Kernel Emissions (SMOKE) model, version 2.6 (Coats and Houyoux, 1996), as it is well suited to process the 2005 NEI. The 2005 NEI are processed by SMOKE to create "model-ready" baseline emissions for 2005, and then each emission year for the future 2046–2050 period are projected by assimilating the transportation sector GFs into SMOKE for each gas (CO, NO, NO_2, NO_x, NH_3, SO_2, and VOCs) and particulate species (PM, EC, and OC) derived from SPEW-Trend. Although the PM, EC, and OC GFs are all similar, SMOKE generates projected emissions of EC and OC that are each model ready to be ingested by the AQM. Considering SMOKE processes many emission sources, types, and fuel classifications for the 2005 NEI, the less-detailed SPEW-Trend GFs for each transportation mode and fuel type are assigned to general SMOKE source classification codes (SCCs), and are also allocated to each U.S. state using SMOKE country, state, county (COSTCY) codes. Table 2 shows how each SPEW-Trend transportation mode and fuel type is generally assigned to a representative SMOKE SCC, while the detailed list of SCC codes and descriptions may be found in the technical support document of EPA (2010), and the references within.

Based on Table 2, growth control input files (i.e., "GCNTL" files) are created and ingested into SMOKE using the "Cntlmat" program, which assigns the GFs with a cross-reference approach similar to those used for chemical speciation and spatial gridding. In this manner, the emissions are projected for each transportation mode available in the 2005 NEI including the National Mobile Inventory Model (NMIM)-based on-road vehicles (on-road), NMIM-based non-road engines (non-road), locomotive and non-C3 commercial marine (alm_no_c3), C3 commercial marine (seca_c3), and aircraft (ptnonipm) modes (EPA, 2010). The locomotive and marine sectors in the 2005 NEI pertain to SPEW-Trend's rail and ship modes, respectively. The other sectors' (i.e., area and point) emissions in the U.S., as well as all of Canada's and Mexico's emissions (i.e., othpt, othar, and othon) stay constant in the future period (2046–2050) to isolate the effects of changing transportation sector emissions over the U.S. The final model-ready emission data sets include projected changes for the 1) on-road vehicles (ORV; on-road only), non-road engines (NRE; non-road only), and 3) total transportation (TT; on-road + non-road + ship + rail + aircraft). Thus we may investigate the individual contributions of ORV and NRE to the TT emission changes. Model-ready ORV, NRE, and TT emissions are then used as input to CMAQ to investigate the impacts on future U.S. air quality in the face of climate change in Part II.

3.4. Transportation emissions over the U.S. By 2046–2050

Fig. 5 shows spatial plots of annual average total 2005 emissions of CO, NO_x, VOC, NH_3, and SO_2, and the absolute changes (future − baseline) in ORV, NRE, and TT for an annual average future 2046–2050 period under the A1B scenario. These model-ready emissions are directly used in CMAQ for the current and future year air quality projections in Part II of this work.

Supplementary Fig. S1 also shows similar annual average spatial plots for the percent change (defined as ((future-baseline)/baseline)*100%), and Supplementary Figs S2 − S5 show percent change for the meteorological winter (January, February, and December (JFD)), spring (March, April, and May (MAM)), summer (June, July, and August (JJA)), and fall (September, October, and November (SON)) seasons. The total emissions for all species in 2005 are the highest east of the Mississippi River and along the west coast of the U.S., except for NH_3, which also exhibits relatively high emissions over an expansive area near the agricultural belts of the Midwest (Fig. 5a–e). The highest emissions of CO, NO_x, VOCs, and SO_2 are found near urban centers that are representative of a high-density of ORV and NRE, as well as near locations of large point sources including both electric generating utilities (EGUs) and non-EGUs (e.g., airports) that are predominant in the eastern half of the U.S. In the U.S., the on-road vehicle and non-road engines account for about 55–60% or more of the total CO and NO_x emissions, and at least 25% of all VOC emissions (DOT, 2016). Most emission variables have minimal seasonal variation for a domain-wide average (differences $\leq$ 10% of the annual average; Figs S2 − S5), except for NH_3, which has over a factor of 2 smaller emissions in the winter (Fig. S2d; 1.1 mol km^{-2} hr^{-1}) compared to the summer (Fig. S4d; 2.9 mol km^{-2} hr^{-1}). A peak in NH_3 emissions due to agricultural (i.e., crop and livestock) sources in the spring and summer seasons is also apparent in other bottom-up emission inventories over the U.S. (e.g., Paulot et al., 2014).

Fig. 6 shows similar spatial plots of annual average total 2005 emissions of PM_{10}, $PM_{2.5}$, primary EC (PEC), and primary organic matter (POM), and their absolute changes in ORV, NRE, and TT emissions.

In general, there are regionally higher total 2005 PM emissions

Table 2
General allocation summary for the SPEW-Trend transportation emissions and fuel type categories related to the SMOKE SCCs used for emission projection assignments. The detailed list of SCC codes and descriptions may be found in U.S. EPA (2010) and the references within.

SPEW-Trend Data		SMOKE Classification	
Transportation Mode	Fuel Type	SCC Code	SCC Description
Non-road	Diesel Fuel	2270000000	Mobile Sources; Off-highway Vehicle Diesel; Compression Ignition Equipment except Rail and Marine
Non-road	Motor Gasoline	2260000000	Mobile Sources; Off-highway Vehicle Gasoline, 2-Stroke; 2-Stroke Gasoline except Rail and Marine
Non-road	Motor Gasoline	2265000000	Mobile Sources; Off-highway Vehicle Gasoline, 4-Stroke; 4-Stroke Gasoline except Rail and Marine
On-road	LDDV	2230001000	Mobile Sources; Highway Vehicles - Diesel; LDDV; Total: All Road Types
On-road	HDDV	2230070000	Mobile Sources; Highway Vehicles - Diesel; All HDDV including Buses; Total: All Road Types
On-road	LDGV	2201001000	Mobile Sources; Highway Vehicles - Gasoline; LDGV; Total: All Road Types
Ship	Total	2280000000	Mobile Sources; Marine Vessels, Commercial; All Fuels; Total, All Vessel Types
Rail	Diesel Fuel	2285000000	Mobile Sources; Railroad Equipment; All Fuels; Total
Aircraft	Aviation Gasoline	2275000000	Mobile Sources; Aircraft; All Aircraft Types and Operations; Total

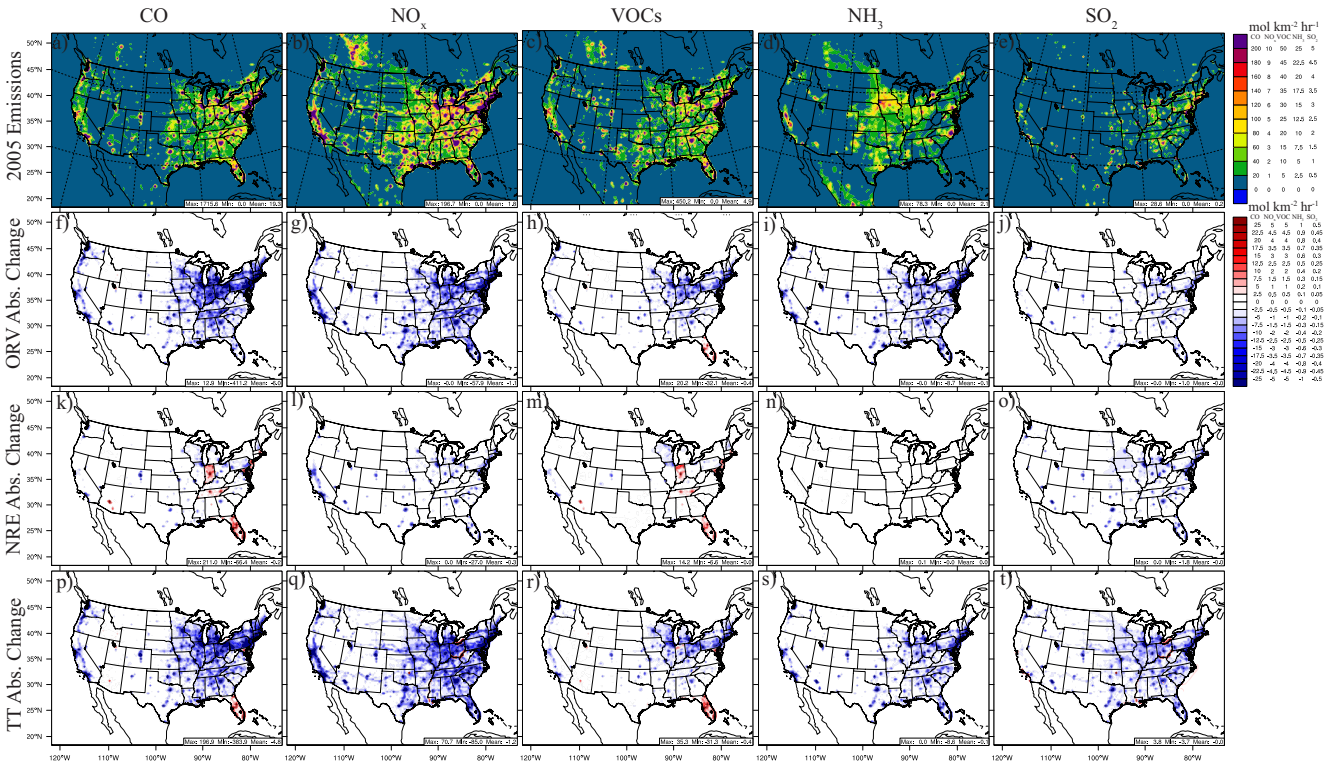

Fig. 5. Spatial plots of annual (January–December) average baseline 2005 emissions (first row; a - e), and future 2046–2050 absolute (future − baseline) changes in ORV (second row; f - j), NRE (third row; k - o), and TT (fourth row; p - t) for CO, NO_x, VOCs, NH_3, and SO_2 emissions under the A1B scenario. Spatial plots of annual average relative percent changes are shown in Supplementary Fig. S1, and seasonal relative percent changes are shown in Supplementary Figs S2 − S5.

in the eastern U.S. compared to more locally enhanced emissions in the western U.S, especially for PEC and POM (Fig. 6a–d). Combined ORV and NRE emissions make up about 5% or less of the total primary PM_{10} and $PM_{2.5}$ emissions from all sectors (DOT, 2016), which is comparably much less than the transportation fractional contribution for gas species in Fig. 5a–e. The spatial distribution of PEC and POM tends to agree with their observations over the U.S. (Hand et al., 2013). The maximum PM emissions are concentrated in urban areas, specifically near highly populated areas that follow the Northeast Corridor, parts of southeast U.S. including Florida, and notably near major cities in the Midwest and western U.S. including California. The high emissions of PM_{10} (Fig. 6a) are more spatially widespread across the U.S. when compared to $PM_{2.5}$ (Fig. 6b). While the total transportation sector comprises about 11% and 12% of the total 2005 $PM_{2.5}$ and POM emissions in the U.S., respectively (Fig. 6b and d), the primary source (~52%) of PEC emissions in the U.S. (Fig. 6c) comes from combustion of transportation sector fuels, especially ORV and NRE, and about 93% of the PEC emissions are from diesel fuel use. (Lamarque et al., 2010; DOE, 2011; EPA, 2012). There is small domain-wide average seasonal variation (within 10–15% of annual average) for all PM emissions (Fig. S6 − S10, panels a–d); however, there are moderate seasonal enhancements apparent in POM emissions over the eastern U.S. during winter and spring (Figs S7d and S8d), and a large seasonal enhancement in POM over the western U.S. during summer (Fig. S9d).

The ORV emissions are projected to decrease for all gas (Fig. 5f–j) and PM emission (Fig. 6e–h) variables across the U.S. by 2046–2050 relative to 2005, except for the VOC emission increases in Florida (Fig. 5h), where the dominating increases in fuel consumption for HDDV (e.g., Figs. 2 and 3a) are larger than the decreases in future emission factor from enhanced emission standards in Florida. The emission decreases are the largest near major urban centers and major interstate highways that connect the most densely populated urban centers (see Fig. S11 for

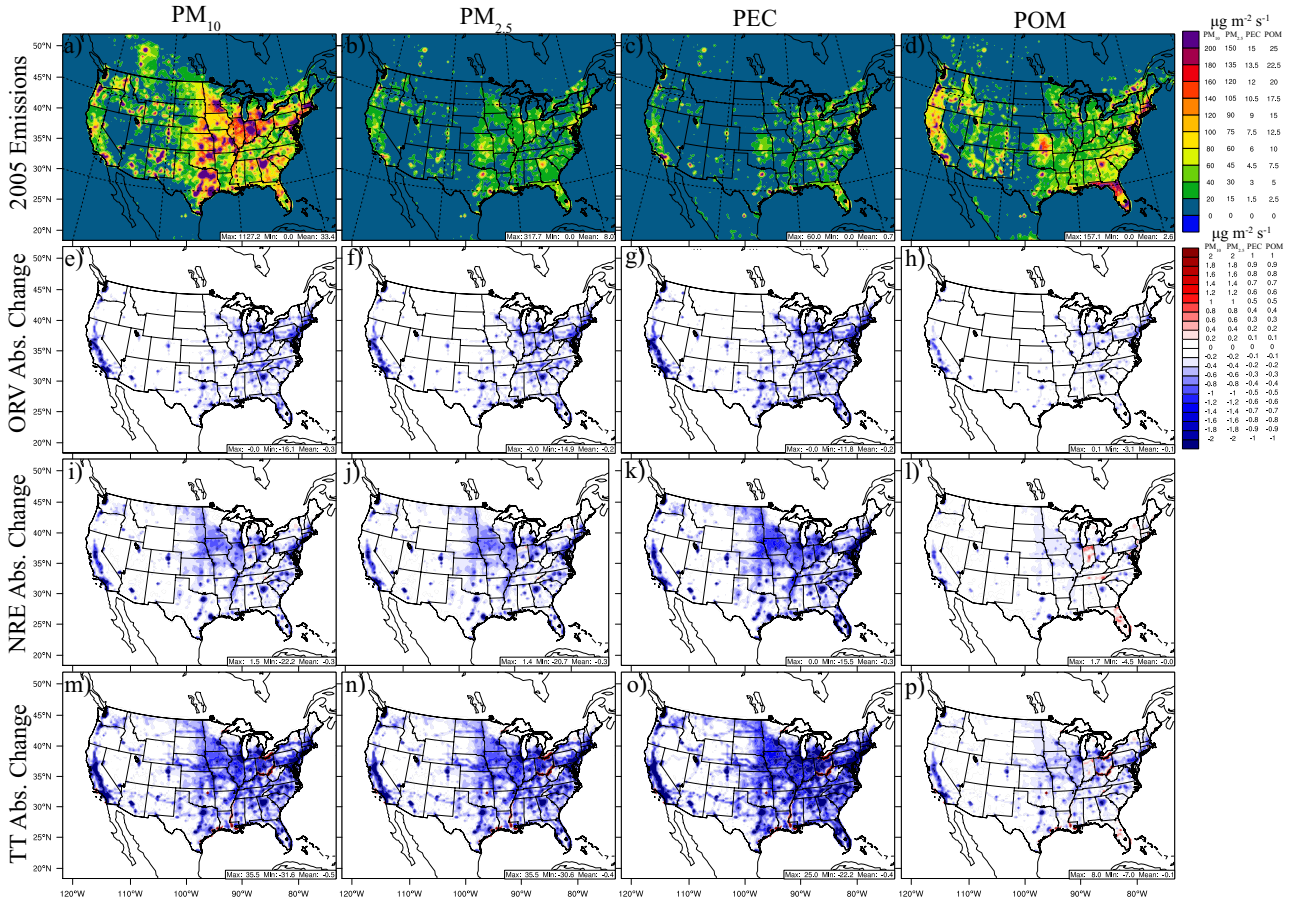

Fig. 6. Same as in Fig. 5, but for PM_{10}, $PM_{2.5}$, PEC, and POM emissions. Spatial plots of annual average relative percent changes are shown in Supplementary Fig. S6, and seasonal relative percent changes are shown in Supplementary Figs S7– S10.

comparison). The annual domain-wide average absolute (percent) changes in ORV emissions of CO, NO_x, VOC, NH_3, and SO_2 are −6.0 (−10.4%), −1.1 (−25.5%), −0.4 (−3.4%), −0.1 (−8.4%), and −0.02 mol km^{-2} hr^{-1} (−9.7%) respectively. For PM_{10}, $PM_{2.5}$, PEC, and POM the absolute (percent) changes in ORV emissions are −0.3 (−0.3%), −0.2 (−1.2%), −0.2 (−10.1%), and −0.1 μg m^{-2} s^{-1} (−1%). The effects of implementation of stringent emission standards and emission reduction technologies (i.e., reduction in the emission factors) offset the increases in fuel consumption, degradation rate, and the superemitter transition rate (Yan et al., 2014), which leads to reductions in emissions for all gas and PM species across the majority of the U.S. There are minimal seasonal fluctuations for ORV emissions changes for both gas and PM variables (Figs S2 – S5).

The NRE emissions predominantly decrease for most gas species (Fig. 5k–o) by 2046–2050 as well, however, there are increases in some U.S. states for CO and VOC (Fig. 5k and m), and there are very small changes in absolute NH_3 emissions across the entire U.S. (Fig. 5n). The NRE emissions of NH_3 are at least an order of magnitude smaller than CO, NO_x, VOC, or SO_2 (not shown), and thus their absolute changes are quite small. The increases in CO and VOC emissions are impacted by GFs >1 for future NRE gasoline emissions over some U.S. states (e.g., Indiana and Florida), in conjunction with fuel consumption increases (Fig. 3a) and monthly/seasonal activity allocation fractions that are used in NRE emissions modeling (EPA, 2005). The seasonal activity allocation leads to considerably more seasonal variability for the NRE emissions compared to ORV emission changes. There is a clear shift in areas of increasing CO and VOC emissions during the winter and spring (Figs S2k and S2m and S3k and S3m), to many areas of decreasing CO and VOC emissions (except in Indiana and Florida) during the summer and fall in the U.S. (Figs S4k and S4m and S5k and S5m). During the winter and spring seasons, there is a larger allocation of certain NRE equipment categories (e.g., snow blowers/snowmobiles in the northern U.S. and recreational marine in the southern U.S.) that use NRE gasoline with enhanced fuel consumption and emissions GFs >1, compared to the summer and fall, where there is a larger allocations to other equipment (e.g., construction and agricultural equipment) that use diesel fuel with emission GFs < 1 due to decreasing emission factors for this transportation mode. NO_x and SO_2 emissions also decrease more significantly in the winter to fall seasons, due to similar NRE monthly/seasonal activity allocations (Figs S2l and S2o and S4l and S4o). The NRE emissions of PM_{10}, $PM_{2.5}$, PEC, and POM decrease in the future (Fig 6i–l), and there is a similar seasonality compared to the gasoline NRE emissions (some increases in winter and mainly decreases in summer). The largest percent decreases are for PEC (Figs S7 – S10). The annual domain-wide average absolute (percent) changes in NRE emissions of CO, NO_x, VOC, NH_3, and SO_2 are −0.2 (−2.2%), −0.3 (−10.3%), −0.1 (−1.5%), 0.0 (0.1%), and −0.03 mol km^{-2} hr^{-1} (−16.4%), respectively. For PM_{10}, $PM_{2.5}$, PEC, and POM the absolute (percent) changes in ORV emissions are −0.3 (−0.3%), −0.3 (−1.5%), −0.3 (−18.2%), and −0.04 μg m^{-2} s^{-1} (−1.4%).

The TT (ORV + NRE + ship + rail + aircraft) emissions show

predominant decreases in all gas and PM emissions by 2046–2050 over CONUS, except in Florida for CO (due to NRE) and VOC (due to both ORV and NRE), and over some major waterways (e.g., Southern Mississippi River and Ohio River Valley) for PM due to large increases in projected ship emissions (Figs 5p–t and 6m–p). Although the absolute differences are small, the percent difference in commercial ship emissions over the coastal ocean regions are also largely positive (Figs S1p – S1t and Figs S6m S6p), which concurs with an overall increase in global ship emissions predicted by 2046–2050 (Yan et al., 2014). The annual domain-wide average absolute (percent) changes in TT emissions of CO, NO_x, VOC, NH_3, and SO_2 are −4.8 (1.8%), −1.2 (−28.6%), −0.4 (−4.1%), −0.1 (−8.3%), and $-0.04\ mol\ km^{-2}\ hr^{-1}$ (−17.6%), respectively. For PM_{10}, $PM_{2.5}$, PEC, and POM the absolute (percent) changes in TT emissions are −0.5 (8.3%), −0.4 (7.2%), −0.4 (−16.6%), and $-0.1\ \mu g\ m^{-2}\ s^{-1}$ (6.9%), respectively. Due to large positive percent changes for offshore ship emission sources for CO and PM (e.g., Figs S1p and S6m-p), there are opposite signs for the domain-wide average absolute and percent changes. Thus, the large percent increases in ship emissions strongly influence the domain-wide average; however, there are predominant decreases in annual absolute TT emissions for all gas and PM species over CONUS by 2046–2050. Overall, the ORV emissions dominate the absolute emission changes for CO, NO_x, VOC, and NH_3 (except in a few states including Florida), and both ORV and NRE modes contribute strongly to PM and SO_2 emission changes. There are clear contributions to the TT decreases from rail emissions, especially for NO_x (Fig. 5q), SO_2 (Fig. 5t), and all PM variables (Fig. 6m–p) near major railways in the western U.S.

4. Model evaluation

A comprehensive meteorological and chemical evaluation is performed for the 2005 WRF_NCEP/CMAQ and WRF_CCSM/CMAQ simulations, where the meteorological performance results for the domain-wide average, spatial and temporal variability, and vertical meteorological profiles and column chemical abundances are provided in Supplementary Section 3. The evaluation consists of a large number of WRF meteorological variables including surface pressure (PSFC), 2-m temperature (T2), 2-m relative humidity (RH2), 10-m wind speed (WSP10), 10-m wind direction (WDR10), downward shortwave radiation at the surface (SWDOWN), planetary boundary layer height (PBLH), and precipitation (PRECIP), as well as CMAQ chemical variables including O_3, CO, NO, SO_2, nitric acid (HNO_3), PM_{10}, $PM_{2.5}$, inorganic $PM_{2.5}$ species (SO_4^{2-}, NO_3^-, NH_4^+), EC, OC, wet deposition of inorganic $PM_{2.5}$ species, and extinction/visibility.

Table 3 shows a general summary of domain-wide annual (January–December) average elevated normalized mean bias (NMB) and normalized mean error (NME) or root mean square error (NRMSE) RMSE, and low Pearson's correlation (R) for select meteorological (T2, RH2, WSP10, SWDOWN, and PRECIP) and chemical (surface O_3 and $PM_{2.5}$, and column O_3 and aerosol optical depth (AOD)) variables, which are based on the full evaluation of the 2005 WRF_CCSM/CMAQ simulation in Supplementary Section 3. The results in Table 3 are used to identify areas of low or high bias, error, and correlation, as well as to highlight some potential implications of the evaluation on assessing and interpreting the WRF_CCSM/CMAQ air quality projections in Part II of this work.

The near-surface meteorological evaluation of the 2005 WRF_NCEP simulation indicates annual average performance statistics near or within acceptable criteria or available literature, thus establishing the 2005 baseline meteorology for this work (Supplementary Section 3 and Table S2). Following a simple bias correction, the 2005 WRF_CCSM demonstrates similar annual average statistics and spatial distribution to WRF_NCEP, although some seasonal average differences exist that are quantified and discussed in Supplementary Section 3. Some aspects of the WRF_CCSM evaluation to note in Table 3 are that 1) minor underpredictions in T2 in parts of CONUS may impact O_3 and $PM_{2.5}$ formation, 2) minor underpredictions in RH2 (due to low moisture transport from CCSM BCONs) in the southeast CONUS may lead to impacts on PRECIP and wet deposition of PM, 3) moderate overpredictions in WSP10 (especially in coastal regions) can impact pollutant transport, PBLH, and pollutant concentrations, 4) minor overpredictions in SWDOWN may impact heat fluxes, PBLH, and O_3 formation, and 5) moderate underpredictions in PRECIP may impact wet deposition of PM in some regions of CONUS (e.g., southeast). Overall however, there is confidence in the ability of the WRF configuration to drive the current- and future-year CMAQ simulations in Part II.

The chemical evaluations indicate that annual NMBs for gas and aerosol species in Table S7 are close to or within the operational evaluation guidelines provided in the literature, while in many areas statistically outperforming previous CMAQ simulations over CONUS. Approximate comparisons of simulated column variables with satellite data also demonstrate a good agreement in spatial distributions and seasonal changes in the tropospheric abundance of CO, NO_2, formaldehyde (HCHO), tropospheric ozone residual (TOR), and AOD (Supplementary Figs S18 - S19, and Table S12). As shown in Table 3, the WRF_CCSM/CMAQ 2005 evaluation tends to have minor overpredictions in surface and column O_3, while

Table 3
Model evaluation summary of potential implications for domain-wide annual (January–December) average elevated NMB and NME or NRMSE, and low R correlation for select meteorological and chemical variables. The summary is based on the full evaluation results of 2005 WRF_CCSM/CMAQ simulation in Supplementary Section 3. Results are an average of all networks analyzed. Responses of yes, no, or borderline (within ±1% for NMB or NME; or within ±0.1 for NRMSE or R) are assigned to each variable, and they are ranked as having minor (= 0–1 yes/borderline), moderate (= 2 yes/borderline), or major (=3 yes/borderline) potential impacts.

Meteorological/Chemical Variable	Elevated NMB (>±20%)?	Elevated NME or NRMSE (>25% or 0.75)?	Low R Correlation (<0.5)?	Potential Implication(s) for Air Quality Projections in Part II (see Supplementary Section 3 for full evaluation)
T2	No.	No.	No	Minor. Underpredictions that impact O_3 and $PM_{2.5}$ formation.
RH2	No.	No.	Borderline.	Minor. Southeast U.S. underpredictions that impact precipitation and wet deposition of PM species.
WSP10	No.	Borderline.	Yes.	Moderate. Coastal overpredictions that affect boundary layer heights and pollutant concentrations.
SWDOWN	No.	Borderline.	No.	Minor. Overpredictions that impact heat fluxes, boundary layer heights, and O_3 formation and concentration.
PRECIP	No.	Yes.	Yes.	Moderate. Underpredictions that impact wet deposition of PM species.
Max 8hr O_3	No.	Yes.	Borderline.	Moderate. Overpredictions in surface O_3 mixing ratios.
24-hr avg. $PM_{2.5}$	Yes.	Yes.	Yes.	Major. Underpredictions in surface $PM_{2.5}$ concentrations.
Tropospheric O_3 Column	Borderline.	No.	No.	Minor. Overpredictions in column O_3 abundance.
Aerosol Optical Depth	Yes.	Yes.	Yes.	Major. Underpredictions in column PM abundance.

exhibiting some major underpredictions in surface and column $PM_{2.5}$. Based on satellite AOD comparisons, the column PM underpredictions are most prevalent in the western CONUS during spring and summer where CMAQ underestimates dust emissions in this region; however, the column PM comparison suffers from uncertainty in both CMAQ predictions and an approximate satellite comparison. The overall good performance results of the chemical evaluations, however, which include good spatial agreement in column gas comparisons against satellite observations (Supplementary Section 3), provide additional confidence in the ability of CMAQ to simulate the projections in air quality variables in Part II.

5. Summary and discussion

Part I of the sequence papers describes the novel Technology Driver Model (TDM) and dynamically downscaled WRFv3.6.1/offline CMAQv5.0.2 (WRF/CMAQ) model system, methodology of transportation emission projections from a dynamic technology model, the Speciated Pollutant Emission Wizard (SPEW)-Trend model (Yan et al., 2014), and the annual and seasonal transportation sector emission changes by 2046–2050 relative to the 2005 National Emissions Inventory (NEI). The emissions are analyzed for the on-road vehicle (ORV), non-road engine (NRE), and total transportation (TT = ORV + NRE + ship + rail + aircraft) modes (Section 2). Based on the emission growth factors (GFs) derived from SPEW-Trend output, there are mainly decreases in ORV and NRE gasoline and diesel emissions for all gas and PM variables, with the exception of NRE gasoline emissions of VOC and PM, and light duty gasoline vehicle (LDGV) emissions of PM. Ship emissions increase for all relevant emission variables due to predicted increases in global emissions from the shipping industry (Yan et al., 2014), while rail and aircraft both increase or decrease depending on the specific emission variables. The significant emission decreases for many species are a result of combined decreases in future emission factors due to the adoption of more stringent regulations in the U.S., and because of decreases in fuel consumption for particular transportation modes (e.g., light-duty diesel vehicles (LDDV) and LDGV); however, the increases in fuel consumption for some transportation modes (e.g., non-road diesel and gasoline) may overcompensate the decreases in future emission factors and lead to increases in future emissions of some species (e.g., CO and VOC) over parts of the U.S.

There are widespread decreases in gas (CO, NO_x, VOC, NH_3, and SO_2) and PM (PM_{10}, $PM_{2.5}$, PEC, and POM) emissions for ORV, NRE, and TT across the continental U.S. by 2046–2050, although there is considerable spatial, seasonal, and inter-transportation mode variability that has not been addressed in previous studies. The NRE emission projections show more spatial and seasonal variability (compared to ORV), with many U.S. states indicating increased CO and VOC emissions due to SPEW-Trend derived GFs >1 for NRE gasoline emissions, which are a result of increases in fuel consumption that are larger than decreases in emission factors, and also in conjunction with monthly/seasonal activity allocation fractions used in NRE emissions modeling. PM emissions widely decrease, although some areas across the domain experience relatively large increases due to increases in ship emissions. The ORV dominate the emission changes for CO, NO_x, VOC, and NH_3, both the ORV and NRE modes have strong contributions to PM and SO_2 emission changes, and there are noticeable contributions from other transportation modes including major railways in the western U.S. for all PM related emissions. Overall, there are predominant decreases in TT emissions, with the exception of ship emissions over waterways.

SPEW-Trend was designed for regional and global emissions, and is a very good methodology for large-scale emission projections, particularly if information is limited. At the U.S. state-level, however, one limitation is that the technology distributions are not distinguished by each state, but rather by future fuel consumption. Thus the early timing of advanced emission standards for states such as California are not represented here. In SPEW-Trend, only emission standards until the U.S. Tier 2 are considered, and after 2007 for light duty vehicles and 2010 for heavy duty vehicles in the U.S., there are no further emission standards included here. It is possible that adoption of more stringent emission standards (and reduction in emission factors) will occur in the long-term for the U.S., and that the transportation emission reductions from SPEW-Trend by 2046–2050 may be underpredicted for some species (Figs. 5 and 6).

Under the TDM approach, Part II of this work applies the transportation emission changes to the dynamically downscaled WRF/CMAQ model system, which employs some of the most advanced regional climate model physical and chemical configuration options available, while investigating the impacts on air quality projections for the U.S. in a changing climate (Campbell et al., 2018). Hence we perform a comprehensive evaluation of the baseline 2005 WRF simulation, which shows that annual biases are close to or within the acceptable criteria for meteorological performance in the literature, and there is an overall good agreement in the 2005 annual statistics and spatial distributions of chemical concentrations from CMAQ against both surface and satellite observations.

There are of course limitations and future aspirations that can help improve the robustness of the emission projections and applications. Such aspects include generating all-sector (including dynamic technology transportation and power/point sectors) emission projections at finer horizontal grid resolutions, and then applying them to online-coupled air quality simulations downscaled from global scales for multiple IPCC scenarios (e.g., A1B vs B2). This work is currently underway (Jena et al., 2018; Wang et al., 2018), where the results will provide a comprehensive TDM approach to investigating emission projections and their impacts on future U.S. air quality at multiple scales. It would also be beneficial to expand the dynamic technology-driven emission projections to other fuels for both the ORV and NRE modes (e.g., compressed or liquefied natural gas) and assess impacts (i.e., uncertainties) from electric vehicles, while at the same time incorporating emission source apportionment changes in the future, such a larger contribution of elemental carbon PM emissions shifting from the transportation sector to the fire sector that includes biomass burning. Finally, some aspects of the projections could be further advanced, such as combining parts of the SPEW-Trend emission projections and the work of Ran et al. (2015). Ran et al. developed a state-to-county level disaggregation and more realistic county-to-model grid allocations (i.e., updated future spatial surrogates used in emission processing), but do not contain the dynamic technology model projections used in this work. To our knowledge, this could lead to some of the most novel emission projections at model grid scale that incorporate dynamic technologically-driven changes.

Acknowledgements

This study is funded by the National Science Foundation Earth System Model (EaSM) program (AGS-1049200) at North Carolina State University, and the United States Department of Agriculture EaSM program (2012-67003-30192) at the University of Chicago/Argonne National Laboratory. The Yellowstone supercomputing services housed in the Computational and Information Systems Lab (CISL) at NCAR were used to run SMOKE for preparing model-ready

emissions. The National Energy Research Scientific Computing Center's (NERSC) Hopper, Edison, and Cori systems were used to perform the WRF and WRF/CMAQ simulations. The meteorological initial and boundary conditions used to drive WRF were provided by NCEP for WRF_NCEP and by NCAR's Community Climate System Model (CCSM) for WRF_CCSM. The initial and boundary conditions from CCSM were further processed by Ruby Leung's group at the Pacific Northwest National Laboratory for dynamical downscaling. We acknowledge the surface observation networks including AIRS-AQS, ARM, CASTNET, CSN, IMPROVE, NADP, NCDENR, PRISM, SEARCH, satellite platforms including OMI, MODIS, MOPITT, and SCIAMACHY, and operational global upper air data observations including those from NOAA/ESRL. All of these observations were downloaded from their respective websites, and were used for the model meteorological, radiative, and chemical evaluations performed in this study. The authors also thank Dr. Kai Wang of North Carolina State University, who provided support for the WRF and WRF/CMAQ simulations, as well as the anonymous reviewers of this manuscript for their insightful comments and edits to help improve the quality of this manuscript.

Appendix A. Supplementary data

Supplementary data related to this article can be found at https://doi.org/10.1016/j.envpol.2018.04.020.

References

Alcamo, J., 1994. Image2.0 integrated modeling of global climate change. In: Joe Alcamo with Papers by the Image Group. Kluwer Academic Publishers, ISBN 0-7923-2860-4.

Avise, J., Chen, J., Lamb, B., Wiedinmyer, C., Guenther, A., Salathe, E., Mass, C., 2009. Attribution of projected changes in US ozone and $PM_{2.5}$ concentrations to global changes. Atmos. Chem. Phys. 8 (4), 15131–15163. https://doi.org/10.5194/acp-9-1111-2009.

Byun, D.W., Schere, K.L., 2006. Review of the governing equations, computational algorithms, and other components of the models- 3 community Multiscale air quality (CMAQ) modeling system. Appl. Mech. Rev. 59, 51–77. https://doi.org/10.1115/1.2128636.

Campbell, P., Yan, F., Lu, Z., Zhang, Y., Streets, D., 2018. Impacts of transportation sector emissions on future U.S. Air quality in a changing climate. Part II: air quality projections and the interplay between emissions and climate change. Environ. Pollut. 238 under revision.

Coats Jr., C.J., Houyoux, M.R., 1996. Fast Emission Modeling with the Sparse Matrix Operator Kernel Emission Modeling System, Presented at the Emission Inventory: Key to Planning, Permits, Compliance, and Reporting. Air & Waste Management Assoc., New Orleans, LA. September 1996.

Dawson, J.P., Racherla, P.N., Lynn, B.H., Adams, P.J., Pandis, S.N., 2009. Impacts of climate change on regional and urban air quality in the eastern United States: role of meteorology. J. Geophys. Res. 114 https://doi.org/10.1029/2008JD009849. D05308.

Department of Energy (DOE), 2011. Emissions of Greenhouse Gases in the United States 2009. DOE/EIA-0573(2009). U.S. Department of Energy, Energy Information Administration, Office of Independent Statistics and Analysis, Washington, DC. Available at: https://www.eia.gov/environment/emissions/ghg_report/ghg_overview.cfm (Last access: June 2016).

Department of Energy (DOE), 2013. Annual Energy Outlook 2013 with Projection to 2040. DOE/EIA-0383(2013). U.S. Department of Energy, Energy Information administration, Office of Integrated Analysis and Forecasting, Washington, DC. Available at: http://www.eia.gov/forecasts/archive/aeo13/index.cfm (Last access: December 2015).

Department of Transportation (DOT), 2016. Transportation Air Quality: Selected Facts and Figures. February 2016. U.S. Department of Transportation, Federal Highway Administration, Washington, D.C.

European Environmental Agency (EEA), 2015. The European environment - state and outlook 2015 (SOER 2015), Global Megatrends. Diverging Glob. Popul. trends.

EPA, 2005. Seasonal and Monthly Activity Allocation Fractions for Nonroad Engine Emissions Modeling, 420-R-05–017. Research Triangle Park, North Carolina.

EPA, 2010. Technical Support Document: Preparation of Emissions Inventories for the Version 4, 2005-based Platform, July 7, 2010. Research Triangle Park, North Carolina.

EPA, 2012. Report to Congress on Black Carbon, Department of the Interior, Environment, and Related Agencies Appropriations Act, 2010, EPA-450/R012–001. Research Triangle Park, North Carolina.

EPA, 2016a. Inventory of U.S. Greenhouse Gas Emissions and Sinks: 1990 – 2014, EPA 430-R-16-002, April 15, 2016. U.S. Environmental Protection Agency, Washington, D.C.

EPA, 2016b. Emissions Inventory for Air Quality Modeling Technical Support Document: Heavy-duty Vehicle Greenhouse Gas Phase 2 Final Rule, EPA-420-R-008, August 2016.

Fann, N., Nolte, C.G., Dolwick, P., Spero, T.L., Brown, A.C., Phillips, S., Anenberg, S., 2015. The geographic distribution and economic value of climate change-related ozone health impacts in the United States in 2030. J. Air Waste Manage. Assoc. 65 (5), 570–580. https://doi.org/10.1080/10962247.2014.996270.

Gao, Y., Fu, J.S., Drake, J.B., Liu, Y., Lamarque, J.-F., 2012. Projected changes of extreme weather events in the eastern United States based on a high resolution climate modeling system. Environ. Res. Lett. 7, 044025. https://doi.org/10.1088/1748-9326/7/4/.

Gao, Y., Fu, J.S., Drake, J.B., Lamarque, J.-F., Liu, Y., 2013. The impact of emission and climate change on ozone in the United States under representative concentration pathways (RCPs). Atmos. Chem. Phys. 13, 9607–9621. https://doi.org/10.5194/acp-13-9607-2013.

Garcia-Menendez, F., Saari, R.K., Monier, E., Selin, N.E., 2015. US air quality and health benefits from avoided climate change under greenhouse gas mitigation. Environ. Sci. Technol. 49 (13), 7580–7588. https://doi.org/10.1021/acs.est.5b01324.

Gonzalez-Abraham, R., Chung, S.H., Avise, J., Lamb, B., Salathé Jr., E.P., Nolte, C.G., Loughlin, D., Guenther, A., Wiedinmyer, C., Duhl, T., Zhang, Y., Streets, D.G., 2015. Atmos. Chem. Phys. 15, 12645–12665. https://doi.org/10.5194/acp-15-12645-2015.

Hand, J.L., Schichtel, B.A., Malm, W.C., Frank, N.H., 2013. Spatial and temporal trends in PM2.5 organic and elemental carbon across the United States. Adv. Meteorology 2013, 367674. https://doi.org/10.1155/2013/367674, 13 pages.

Hogrefe, C., Lynn, B., Civerolo, K., Ku, J.-Y., Rosenthal, J., Rosenzweig, C., Goldberg, R., Gaffin, S., Knowlton, K., Kinney, P.L., 2004. Simulating changes in regional air pollution over the eastern United States due to changes in global and regional climate and emissions. J. Geophys. Res. 109 https://doi.org/10.1029/2004JD004690. D22301.

International Energy Agency (IEA), 2014. Harnessing Electricity's potential. Energy Technol. Perspect. 2014, 382.

Jacob, D.J., Winner, D.A., 2009. Effect of climate change on air quality. Atmos. Environ. 43, 51–63. https://doi.org/10.1016/j.atmosenv.2008.09.051.

Jena, C., Zhang, Y., Wang, K., Campbell, P., Yan, F., Lu, Z., Streets, D., 2018. Decadal Application of WRF/Chem under Current and Future Climate/emission Scenarios, Part II: Impacts of Climate and Emission Changes on Regional Meteorology and Air Quality in preparation.

Lam, Y.F., Fu, J.S., Wu, S., Mickley, L.J., 2011. Impacts of future climate change and effects of biogenic emissions on surface ozone and particulate matter concentrations in the United States. Atmos. Chem. Phys. 11, 4789–4806. https://doi.org/10.5194/acp-11-4789-2011.

Lamarque, J.-F., Bond, T.C., Eyring, V., Granier, C., Heil, A., Klimont, Z., Lee, D., Liousse, C., Mieville, A., Owen, B., Schultz, M.G., Shindell, D., Smith, S.J., Stehfest, E., Aardenne, J.V., Cooper, O.R., Kainuma, M., Mahowald, N., McConnell, J.R., Naik, V., Rishi, K., Vuuren, D.P.V., 2010. Historical (1850-2000) gridded anthropogenic and biomass burning emissions of reactive gases and aerosols: methodology and application. Atmos. Chem. Phys. 10, 7017–7039.

Leung, L.R., Kuo, Y.H., Tribbia, J., 2006. Research needs and directions of regional climate modeling using WRF and CCSM, B. Am. Meteorol. Soc. 87, 1747–1751.

Liu, C., Lin, Z., 2017. How uncertain is the future of electric vehicle market: results from Monte Carlo simulations using a nested logit model. Int. J. Sustain. Transp. 11 (4), 237–247. https://doi.org/10.1080/15568318.2016.1248583.

Nakicenovic, N., Alcamo, J., Davis, G., de Vries, B., Fenhann, J., Gaffin, S., Gregory, K., Grübler, A., Jung, T.Y., Kram, T., La Rovere, E.L., Michaelis, L., Mori, S., Morita, T., Pepper, W., Pitcher, H., Price, L., Riahi, K., Roehrl, A., Rogner, H., Sankovski, A., Schlesinger, M., Shukla, P., Smith, S., Swart, R., van Rooijen, S., Victor, N., Zhou, D., 2000. Special Report on Emissions Scenarios: a Special Report of Working Group III of the Intergovernmental Panel on Climate Change. Cambridge University Press, Cambridge, New York.

Nolte, C., Gilliland, A.B., Hogrefe, C., Mickley, L.J., 2008. Linking global to regional models to assess future climate impacts on surface ozone levels in the United States. J. Geophys. Res. 113. D14307. https://doi.org/10.1029/2007JD008497.

Paulot, F., Jacob, D.J., Pinder, R.W., Bash, J.O., Travis, K., Henze, D.K., 2014. Ammonia emissions in the United States, European Union, and China derived by high-resolution inversion of ammonium wet deposition data: interpretation with a new agricultural emissions inventory (MASAGE_NH3). J. Geophys. Res. Atmos. 119, 4343–4364. https://doi.org/10.1002/2013JD021130.

Penrod, A., Zhang, Y., Wang, K., Wu, S.-Y., Leung, L.R., 2014. Impacts of future climate and emission changes on U.S. air quality. Atmos. Environ. 89, 533–547. https://doi.org/10.1016/j.atmosenv.2014.01.001.

Pye, H.O.T., Liao, H., Wu, S., Mickley, L.J., Jacob, D.J., Henze, D.K., Seinfeld, J.H., 2009. Effect of changes in climate and emissions on future sulfate-nitrate-ammonium aerosol levels in the United States. J. Geophys. Res. 114 https://doi.org/10.1029/2008JD010701. D01205.

Ran, L., Loughlin, D.H., Yang, D., Adelman, Z., Baek, B.H., Nolte, C.G., 2015. ESP v2.0: enhanced method for exploring emission impacts of future scenarios in the United States – addressing spatial allocation. Geosci. Model Dev. 8, 1775–1787. https://doi.org/10.5194/gmd-8-1775-2015.

Rudokas, J., Miller, P.J., Trail, M.A., Russell, A.G., 2015. Regional air quality management aspects of climate change: impact of climate mitigation options on

regional air emissions. Environ. Sci. Technol. 49 (8), 5170–5177. https://doi.org/10.1021/es505159z.
Skamarock, W.C., Klemp, J.B., Dudhia, J., Gill, D.O., Barker, D.M., Duda, M.G., Huang, X.-Y., Wang, W., Powers, J.G., 2008. A description of the Advanced Research WRF version 3. Natl. Cent. Atmos. Res. Tech. Note 113. US7/TN-475+STR.
Skamarock, W.C., Klemp, J.B., 2008. A time-split nonhydrostatic atmospheric model for weather research and forecasting applications. J. Comput. Phys. 227, 3465–3485.
Tai, A.P.K., Mickley, L.J., Jacob, D.J., 2010. Correlations between fine particulate matter (PM2.5) and meteorological variables in the United States: implications for the sensitivity of PM2.5 to climate change. Atmos. Environ. 44 (32), 3976–3984. https://doi.org/10.1016/j.atmosenv.2010.06.060.
Tao, Z., Williams, A., Huang, H.-C., Caughey, M., Liang, X.-Z., 2007. Sensitivity of U.S. surface ozone to future emissions and climate changes. Geophys. Res. Lett. 34 https://doi.org/10.1029/2007GL029455. L08811.
Trail, M., Tsimpidi, A.P., Liu, P., Tsigaridis, K., Hu, Y., Nenes, A., Russell, A.G., 2013. Downscaling a global climate model to simulate climate change over the US and the implication on regional and urban air quality. Geosci. Model Dev. 6 e1445. https://doi.org/10.5194/gmd-6-1429-2013.
Wang, J., Kotamarthi, V.R., 2015. High-resolution dynamically downscaled projections of precipitation in the mid and late 21st century over North America. Earth's Future 3. https://doi.org/10.1002/2015EF00304.
Wang, K., Jena, C., Zhang, Y., Campbell, P., Yan, F., Lu, Z., Streets, D., 2018. Decadal Application of WRF/Chem under Current and Future Climate/emission Scenarios, Part I in preparation.
Weaver, C.P., Coauthors, 2009. A preliminary synthesis of modeled climate change impacts on U.S. Regional ozone concentrations. Bull. Amer. Meteor. Soc. 90, 1843–1863. https://doi.org/10.1175/2009BAMS2568.1.
Yahya, K., Wang, K., Campbell, P., Chen, Y., Glotfelty, T., He, J., Pirhalla, M., Zhang, Y., 2017a. Decadal application of WRF/chem for regional air quality and climate modeling over the U.S. Under the representative concentration pathways scenarios. Part 1: model evaluation and impact of downscaling. Atmos. Environ. 152, 562–583. https://doi.org/10.1016/j.atmosenv.2016.12.029.
Yahya, K., Campbell, P., Zhang, Y., 2017b. Decadal application of WRF/chem for regional air quality and climate modeling over the U.S. Under the representative concentration pathways scenarios. Part 2: current vs. Future simulations. Atmos. Environ. 152, 584–604. https://doi.org/10.1016/j.atmosenv.2016.12.028.
Yan, F., Winijkul, E., Jung, S., Bond, T.C., Streets, D.G., 2011. Global emission projections of particulate matter (PM): I. Exhaust emissions from on-road vehicles. Atmos. Environ. 45, 4830–4844. https://doi.org/10.1016/j.atmosenv.2011.06.018.
Yan, F., Winijkul, E., Streets, D.G., Lu, Z., Bond, T.C., Zhang, Y., 2014. Global emission projections for the transportation sector using dynamic technology modeling. Atmos. Chem. Phys. 14 https://doi.org/10.5194/acp-14-5709-2014, 5790 – 5733.